

DISPERSION OF GRAPHENE OXIDE AND ITS FLAME RETARDANCY EFFECT ON EPOXY NANOCOMPOSITES*

Zhou Wang^a, Xiu-zhi Tang^a, Zhong-zhen Yu^{a**}, Peng Guo^b, Huai-he Song^{b**} and Xu-sheng Du^c

^a Beijing Key Laboratory on Preparation and Processing of Novel Polymeric Materials,
Department of Polymer Engineering, College of Materials Science and Engineering,
Beijing University of Chemical Technology, Beijing 100029, China

^b State Key Laboratory of Chemical Resource Engineering, College of Materials Science and Engineering,
Beijing University of Chemical Technology, Beijing 100029, China

^c Centre for Advanced Materials Technology, School of Aerospace, Mechanical and Mechatronics Engineering J07,
The University of Sydney, Sydney, NSW 2006, Australia

Abstract Graphene oxide was prepared by ultrasonication of completely oxidized graphite and used to improve the flame retardancy of epoxy. The epoxy/graphene oxide nanocomposite was studied in terms of exfoliation/dispersion, thermal stability and flame retardancy. X-ray diffraction and transmission electron microscopy confirmed the exfoliation of the graphene oxide nanosheets in epoxy matrix. Cone calorimeter measurements showed that the time to ignition of the epoxy/graphene oxide nanocomposite was longer than that of neat epoxy. The heat release rate curve of the nanocomposite was broadened compared to that of neat epoxy and the peak heat release rate decreased as well.

Keywords: Graphene oxide; Epoxy; Nanocomposite; Flame retardancy.

INTRODUCTION

Graphene has a 2-dimensional crystalline structure and consists of only one layer of carbon atoms, and exhibits many functionalities including high stiffness, high thermal and electrical conductivities^[1–4]. Much attention has been paid to the preparation of polymer nanocomposites using graphene as a functional nanofiller. Ruoff *et al.*^[5] prepared polystyrene/graphene nanocomposites with a low percolation threshold of 0.1 vol%. When the loading of graphene increased to 2.5 vol%, the electrical conductivity was as high as 2 S/m. Wang *et al.*^[6] blended graphene oxide with epoxy, the obtained epoxy nanocomposites showed excellent thermal conductivities. The nanocomposite with 5 wt% of graphene oxide showed 4-fold increment of thermal conductivity compared to epoxy matrix. Rafiee *et al.*^[7] compared the mechanical reinforcement of thermally exfoliated graphene nanosheets, single-walled carbon nanotubes and multi-walled carbon nanotubes on the epoxy matrix at a fixed nanofiller content of 0.1 wt%. The results indicated that graphene nanosheets significantly out-performed carbon nanotubes in terms of Young's modulus, tensile strength and fracture toughness.

The graphite oxide (oxidized natural graphite before thermal or ultrasonic exfoliation) has been used as a flame retardant of polymers due to its layered structure and expandable feature^[8–10]. Wilkie *et al.*^[9] prepared polyamide 6 composites by melt compounding with different natural graphite, graphite oxide and thermally

* This work was financially supported by the National Natural Science Foundation of China (No. 50873006), Program for New Century Excellent Talents in Universities, Ministry of Education of China (NCET-08-0711).

** Corresponding author: Zhong-zhen Yu (于中振), E-mail: yuzz@mail.buct.edu.cn

Huai-he Song (宋怀河), E-mail: songhh@mail.buct.edu.cn

Received April 21, 2010; Revised June 7, 2010; Accepted June 17, 2010

doi: 10.1007/s10118-011-1037-7

expanded graphite. The graphite oxide composites showed superior flame retardancy compared to polyamide 6/clay nanocomposites. Li and Qu^[10] investigated synergistic effect of graphite oxide and halogen-free flame retardant on flame retardancy of ethylene vinyl acetate. The effect of anti-flaming was associated with the particle size and the expansion ratio of the graphite oxide. Yang *et al.*^[11] prepared high-density rigid polyurethane foam composites filled with graphite oxide. Interestingly, when the loading of the graphite oxide was more than 10 wt%, the composites reached V-0 rating of the UL-94 vertical burning test. Recently, Higginbotham *et al.*^[12] studied flame retardancy of graphite oxide nanocomposites using polycarbonate, acrylonitrile butadiene styrene and high-impact polystyrene as matrices. Cone calorimeter measurements of the nanocomposites revealed that the total heat release and peak heat release of the three nanocomposites decreased obviously due to the presence of the graphite oxide.

The efficiency of graphite oxide on flame retardancy of polymers depends on many factors. One is the oxidation extent of natural graphite. Complete oxidation is a prerequisite for highest expansion volume during combustion. The other is the dispersion quality of the graphite oxide. Homogeneous dispersion provides efficient barrier effect on mass and heat transfer between gaseous- and condensed-phases. In addition, to avoid thermal degradation of graphite oxide during compounding with polymers, the compounding temperature should be lower than the degradation temperature of graphite oxide (180–250°C)^[13]. As such, epoxy was chosen as polymer matrix in the present study as its curing temperature can be lower than 180°C. To maximize the barrier efficiency, natural graphite was completely oxidized and ultrasonically exfoliated into graphene oxide nanosheets. The epoxy/graphene oxide nanocomposite was studied in terms of exfoliation/dispersion, thermal stability and flame retardancy.

EXPERIMENTAL

Materials

Natural graphite flakes with an average diameter of 48 µm were provided by Huadong Graphite Factory (Pingdu, China). Concentrated sulfuric acid (95%–98%), concentrated nitric acid (68%) and hydrochloric acid (36%–38%) were bought from Beijing Chemical Factory (China). Potassium chlorate (99.5%) was purchased from Fuchen Chemical Factory (Tianjin, China). The epoxy used here was a bisphenol-A based epoxy with a trade name of Epoxy 828 (Ashell, Britain) and the curing agent was 2-ethyl-4-methylimidazole (2E4M) (Tianjin, China).

Synthesis of Graphite Oxide

Graphite oxide was prepared by oxidizing natural graphite flakes in a solution of sulfuric acid, nitric acid and potassium chlorate for 96 h based on the work of Aksay and co-workers^[14, 15]. First, concentrated sulfuric acid and concentrated nitric acid were mixed during mechanical stirring in a flask with an ice bath. Several minutes later, graphite flakes were added into the flask. With vigorous stirring, graphite flakes were dispersed well in the acid mixture to form a fine suspension. Then, potassium chlorate was added into the suspension. To avoid sudden heat release, potassium chlorate was added slowly. The suspension reacted for 96 h at room temperature. After the reaction, a mass of deionized water was used to dilute the suspension. Graphite oxide precipitate was obtained by centrifuging and was washed with HCl solution (5%) to eliminate sulphate ions. Barium chlorate was used to test whether sulphate ions were eliminated or not. After the test was negative, the graphite oxide was washed by deionized water until the pH value was neutral and dried in a vacuum oven at 80°C for 24 h.

Preparation of Graphene Oxide

The dried graphite oxide was grinded into fine powders and mixed with deionized water in a beaker, and the pH value of the mixture was adjusted into 8 by ammonia. The suspension was then subject to intense ultrasonic treatment using a JY99-2 DN ultrasonicator (Ningbo Scientz Biotechnology Co., Ltd., China). During the intense sonication, the graphite oxide powders should be exfoliated into graphene oxide nanosheets, and a brown solution was formed in the beaker. The graphene oxide nanosheets were obtained by filtration and then dried in a vacuum oven at 80°C for 24 h.

Preparation of Epoxy/Graphene Oxide Nanocomposites

Graphene oxide powder was first dispersed in acetone with the help of an IKA T18 homogenizer (Germany). Epoxy monomer liquid was heated to 80°C in an oil bath to reduce its viscosity. Then, the acetone solution of graphene oxide was added into the epoxy at 80°C under high speed stirring. After the acetone was evaporated, the mixture was further degassed in a vacuum oven at 80°C. Curing agent 2E4M was added, and then the mixture was sonicated at high amplitude for 30 seconds. Finally, the mixture was poured into a teflon mould to cure at 80°C for 1 h followed by post cure at 120°C for 3 h.

Characterizations

X-ray diffraction (XRD) scans of natural graphite, graphite oxide and graphene oxide were carried out on a Rigaku D/Max 2500 X-ray diffractometer (Japan) with Cu K α radiation ($\lambda = 0.154$ nm) at a generator voltage of 40 kV and a generator current of 50 mA. The scanning was from 5° to 30° with a speed of 2.4 (°)/min and a step size of 0.002°. The natural graphite and graphite oxide were analyzed using a ThermoVG RSCAKAB 250X X-ray photoelectron spectroscopy (Britain). Thermal stabilities of graphite oxide and its epoxy nanocomposite were measured on a NETZSCH TG-209C thermogravimetric analyzer (Germany) with the heating rate of 5 K/min under air atmosphere. The graphene oxide was characterized with a Thermo Nicolet NEXUS Fourier-transform infrared spectroscopy (USA). To study the dispersion of the graphene oxide nanosheets in epoxy matrix, ultra-thin sections in the range of 60–90 nm in thickness were cryogenically cut with a diamond knife at room temperature using a Leica Ultracut S microtome with a cutting speed of 0.2 mm/s. Sections were collected on formvar/carbon coated 400-mesh copper grids. The thin sections were observed using a Philips CM12 transmission electron microscope (the Netherlands) at an accelerating voltage of 120 kV. The combustion behavior of the nanocomposite was measured on an FTT cone calorimeter (Britain) with the heat flux of 50 kW/m².

RESULTS AND DISCUSSION

Characterization of Graphite Oxide and Graphene Oxide

Complete oxidation of graphite is a prerequisite to ensure complete exfoliation of graphite oxide. Figure 1 shows the XRD patterns of natural graphite, graphite oxide and graphene oxide. Natural graphite exhibits a strong and sharp peak at 26.5° in Fig. 1(a), indicating a highly ordered structure. After oxidation of 96 h, the diffraction peak at 26.5° disappears and a new peak at 12.3° with an intra-gallery spacing of 0.72 nm appears^[16–18], which confirms the complete oxidization of natural graphite. Interestingly, no peak appears after the graphite oxide was exfoliated by ultrasonication in Fig. 1(c).

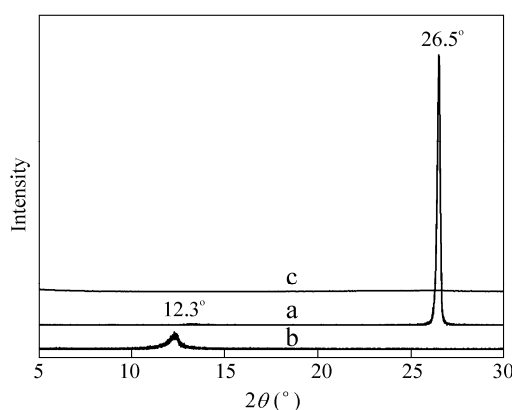


Fig. 1 X-ray diffraction patterns of (a) natural graphite, (b) graphite oxide and (c) graphene oxide

Figure 2 shows the X-ray photoelectron spectroscopy (XPS) curves of natural graphite, graphite oxide and graphene oxide. The C1s XPS spectrum of natural graphite in Fig. 2(a) demonstrates that the C atoms exist as non-oxygenated ring C (284.8 eV) in natural graphite. However, in the C1s XPS spectra of the graphite oxide and graphene oxide, there are four different fitted curves, corresponding to four functional groups: the non-oxygenated ring C (284.8 eV), the C in C—O bonds (286.2 eV), the C in carbonyl groups (C=O, 287.8 eV) and the carboxylate carbon (O—C=O, 289.0 eV)^[19]. The analyses of the C1s XPS peaks reveal that the weight percentage of non-oxygenated ring C in natural graphite is 99%, much higher than 56% of the graphite oxide and the graphene oxide. The reactive groups of the graphite oxide and graphene oxide are also reflected in their FT-IR spectra (Fig. 3). Compared to natural graphite, graphite oxide and graphene oxide exhibit two peaks at 1560 and 1719 cm^{-1} , which are attributed to the benzene ring and carboxyl groups^[20], and one peak at 1223 cm^{-1} is resulted from the C—O group and the peaks at 826, 934 and 1027 cm^{-1} are caused by the epoxide group^[21, 22]. The XPS and FT-IR characterizations indicate that the reactive groups in graphite oxide and graphene oxide are the same, which means that the ultrasonic treatment did not affect the oxygen-containing groups in the graphite oxide.

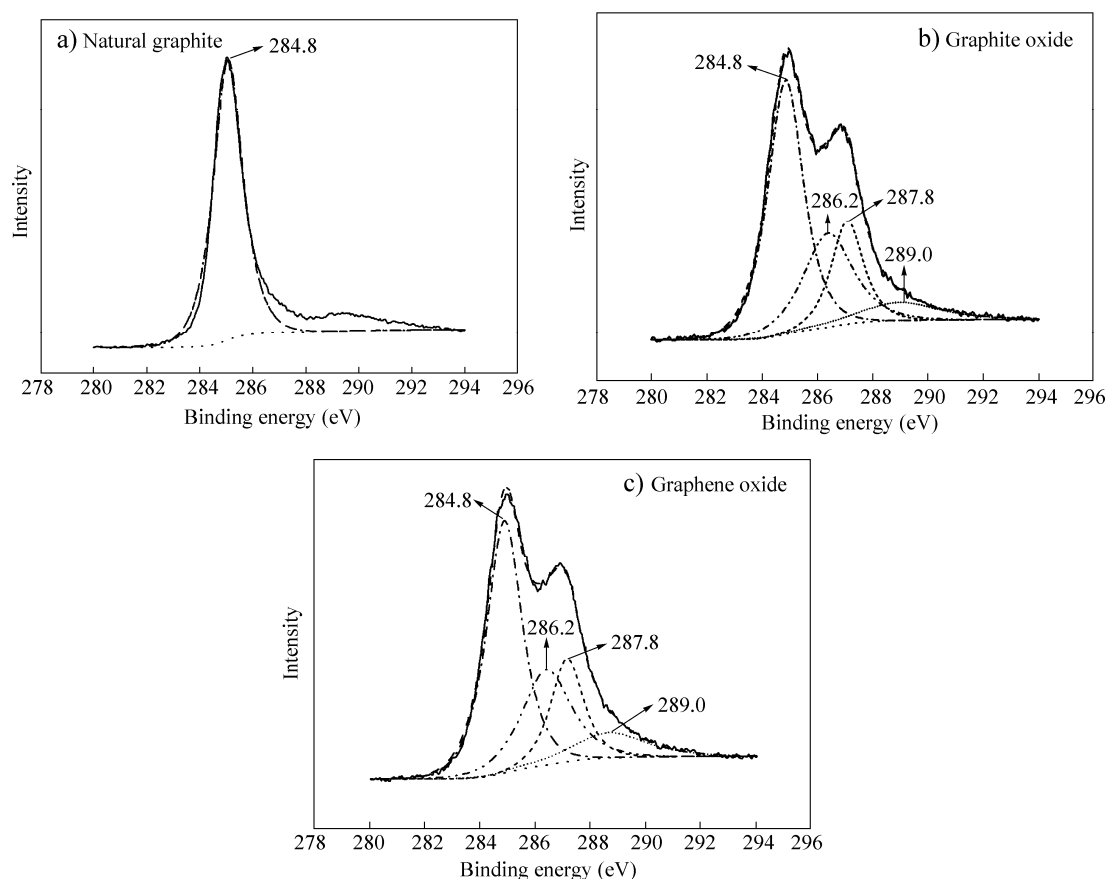


Fig. 2 X-ray photoelectron spectroscopy spectra of (a) natural graphite, (b) graphite oxide and (c) graphene oxide

The thermal stability of natural graphite, graphite oxide and graphene oxide was characterized by TGA. As shown in Fig. 4(a), natural graphite is thermally stable before 600°C and has an exothermic peak at 837°C. Compared with natural graphite, the thermal stabilities of graphite oxide and graphene oxide are low. The primary mass loss of graphite oxide with an exothermic peak at 250°C is mainly due to the decomposition of the oxygen-functional groups of the graphite oxide, generating gas of carbon dioxide^[15]. It is believed that the

generation of non-flammable carbon dioxide benefits the efficiency of flame retardancy. The mass loss with an exothermic peak at 634°C results from the combustion of the carbon skeleton in the graphite oxide^[23]. The TGA curve of graphene oxide is similar to that of the graphite oxide. However, the temperature of the second exothermic peak is lower than that of the graphite oxide, which is possibly related to the exfoliated structure of the graphene oxide. The low thermal stability of graphene oxide is a drawback for its application as a flame retardant of polymers that have high melt compounding temperature over 200°C.

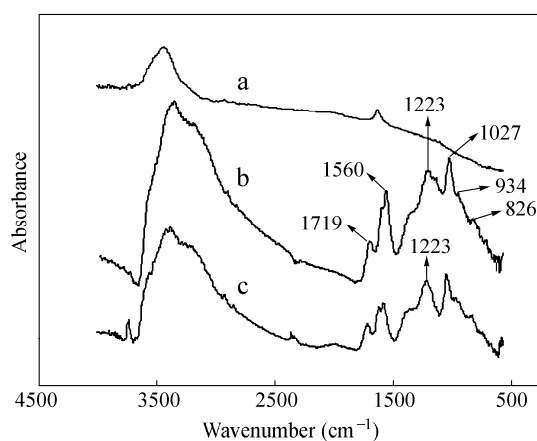


Fig. 3 FT-IR spectra of (a) natural graphite, (b) graphite oxide and (c) graphene oxide

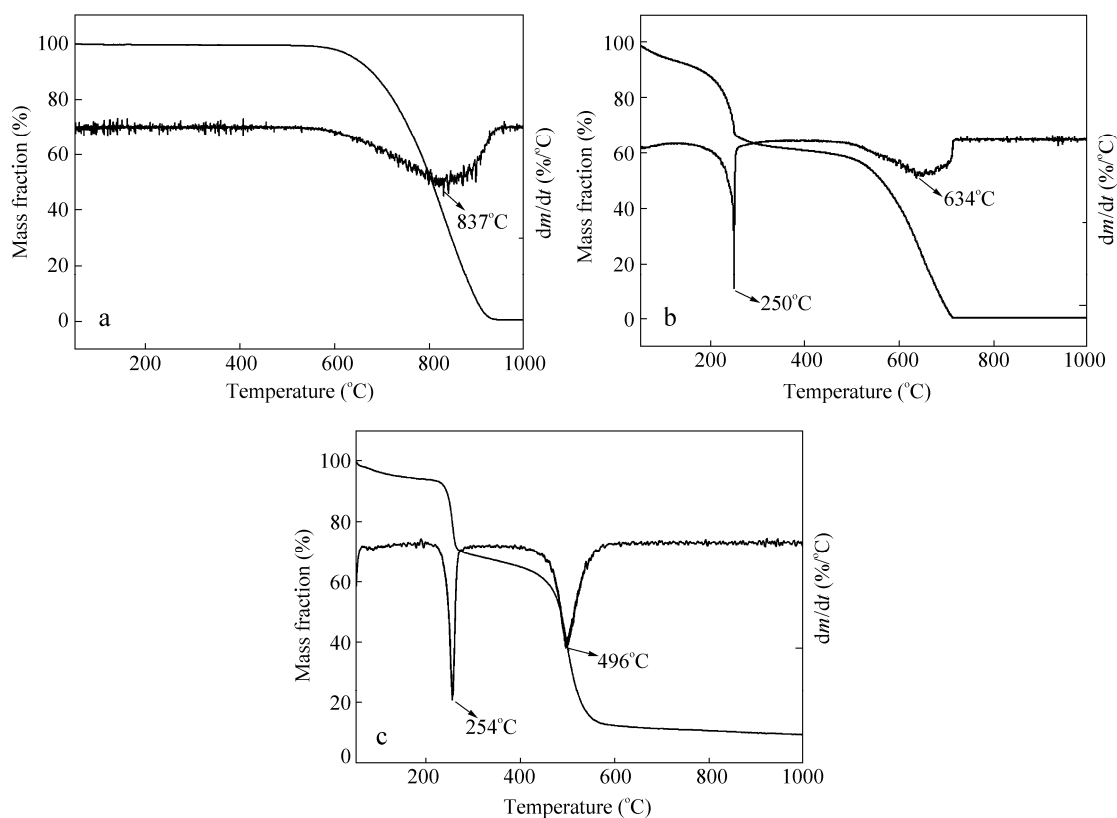


Fig. 4 TGA curves of (a) natural graphite, (b) graphite oxide and (c) graphene oxide

Morphology and Thermal Stability of Epoxy/Graphene Oxide Nanocomposites

Figure 5 shows XRD patterns of neat epoxy and epoxy/2 wt% graphene oxide nanocomposite. Neat epoxy resin exhibits only one broad peak at 18.5° , reflecting its amorphous feature. Interestingly, the nanocomposite also has this peak only and does not exhibit any other peak, indicating an exfoliated feature of graphene oxide in epoxy matrix^[24]. To directly confirm the exfoliation of the graphene oxide nanosheets, Figure 6 shows a TEM microphotograph of the epoxy nanocomposite with 2 wt% of graphene oxide. It is clear that the graphene oxide nanosheets are well dispersed in epoxy matrix.

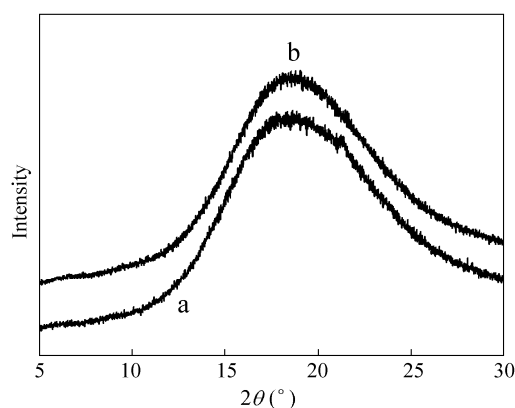


Fig. 5 XRD patterns of (a) epoxy and (b) epoxy/2 wt% graphene oxide nanocomposite

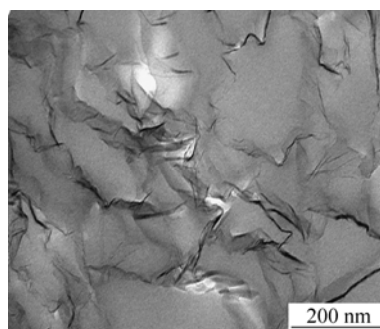


Fig. 6 TEM microphotograph of epoxy/2 wt% graphene oxide nanocomposite

Figure 7 shows TGA curves of neat epoxy and its graphene oxide nanocomposites. The data collected from the curves are listed in Table 1. Neat epoxy exhibits an exothermal peak at 445°C during the heating process. Interestingly, the $T_{5\%}$ of epoxy is 365.7°C while the $T_{5\%}$ values of the nanocomposites with 1 wt% and 2 wt% graphene oxide are 408.7°C and 401.4°C , respectively. The results demonstrate that the addition of graphene oxide increased the temperature at which the mass loss reached 5 wt%. The maximum degradation temperatures (T_m) of the epoxy nanocomposites with 1 wt% and 2 wt% graphene oxide are also higher than that of neat epoxy. These results prove that the presence of graphene oxide improves thermal stability of the epoxy.

Table 1. Thermal degradation temperatures of epoxy and its graphene oxide nanocomposites

Sample	$T_{5\%}$ ($^\circ\text{C}$) ^a	T_m ($^\circ\text{C}$) ^b
Epoxy	365.7	445
Epoxy/1 wt% graphene oxide	408.7	446
Epoxy/2 wt% graphene oxide	401.4	448

^a $T_{5\%}$ is defined as the temperature at 5% mass loss occurred;

^b T_m is defined as the temperature at the maximum mass loss from the TGA curve.

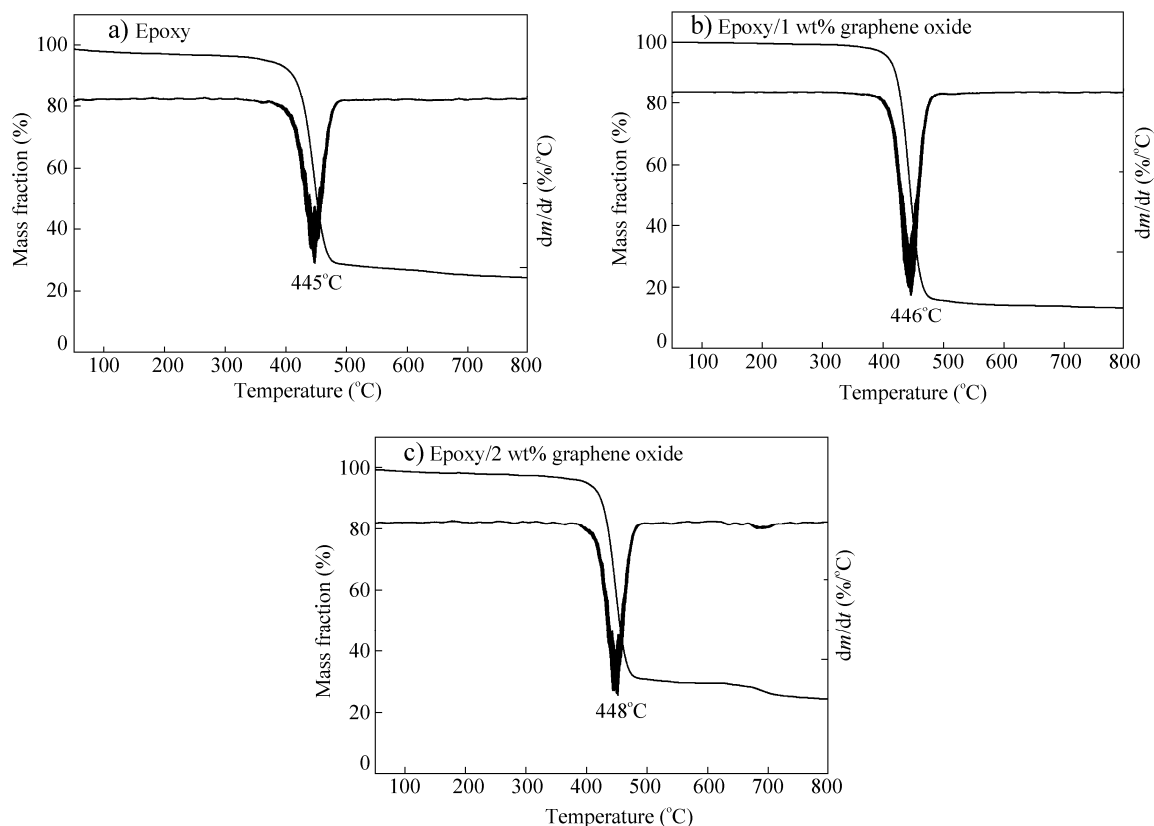


Fig. 7 TGA curves of neat epoxy and its graphene oxide nanocomposites

Flame Retardancy of Epoxy/Graphene Oxide Nanocomposite

The epoxy and its nanocomposite were characterized with cone calorimeter at a heat flux of 50 kW/m^2 . The heat release rates (HRR) of neat epoxy and its nanocomposite with 1 wt% graphene oxide are shown in Fig. 8, and the values of the related parameters are listed in Table 2. It is interesting that the time to ignition of the graphene oxide nanocomposite is longer than that of neat epoxy. The delayed burning may be attributed, in part, to the generated CO_2 gas when the sample was heated, and in part, to the enhanced thermal conductivity of thermally reduced graphene oxide, which benefits the heat dissipation in a more large volume of the tested sample. It is also seen that the HRR curve of the nanocomposite is broadened compared to that of neat epoxy, and the peak heat release rate (PHRR) decreases as well. In addition, the peak SEA value declines sharply, indicating that the graphene oxide nanosheets had a fairly positive effect on the smoke suppression. The mean CO yield is also reduced by *ca.* 17.6%. It should be noted that 1 wt% graphene oxide was converted to even less amount of graphene nanosheets after being heated and burned, implying that 1 wt% graphene oxide was too low to play a significant role as a barrier of mass and heat transfer, which is in consistent with the less significant reduction of the heat release rate. It is expected that high contents of graphene oxide in the epoxy matrix would exhibit a better flame retardancy effect during combustion by forming a continuous and stable barrier char and generating more non-flammable gases.

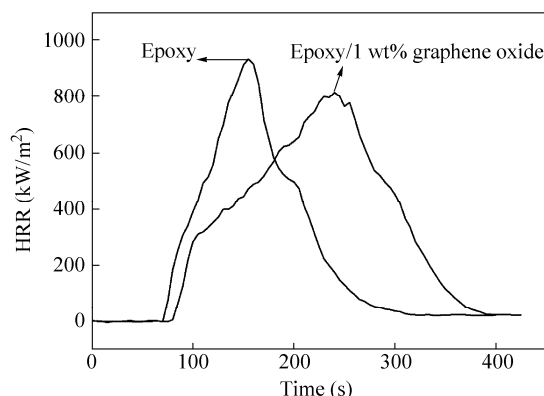


Fig. 8 Heat release rate curves of neat epoxy and epoxy/1 wt% graphene oxide nanocomposite

Table 2. Results of the cone calorimeter measurements at a heat flux of 50 kW/m²

Sample	Epoxy	Epoxy/1 wt% graphene oxide
Time to ignition (s)	66	76
Mean MLR (g/s)	0.10	0.16
THR (MJ/m ²)	95	133
Peak specific extinction area (m ² /kg)	4794	2078
Mean specific extinction area (m ² /kg)	1185	1205
Mean CO yield (kg/kg)	0.07	0.06
Mean CO ₂ yield (kg/kg)	1.9	1.9

CONCLUSIONS

The graphene oxide was prepared by ultrasonication of fully oxidized natural graphite and filled with epoxy resin. XRD and TEM confirmed the exfoliation of the graphene oxide nanosheets in epoxy matrix. Cone calorimeter measurements showed that the time to ignition of the epoxy/graphene oxide nanocomposite was longer than that of neat epoxy. The heat release rate curve of the nanocomposite was broadened compared to that of neat epoxy, and the peak heat release rate decreased as well. Further study will focus on the effect of graphene oxide content on flame retardancy of the epoxy nanocomposites.

REFERENCES

- Si, Y.C. and Samulski, E.T., *Nano Lett.*, 2008, 8: 1679
- Rafiee, M.A., Rafiee, J., Srivastava, I., Wang, Z., Song, H.H., Yu, Z.Z. and Koratkar, N., *Small*, 2010, 6: 179
- Elias, D.C., Nair, R.R., Mohiuddin, T.H.G., Morozov, S.V., Blake, P., Halsall, M.P., Ferrari, A.C., Boukhalov, D.W., Katsnelson, M.I., Geim, A.K. and Novoselov, K.S., *Science*, 2009, 323: 610
- Zhou, S.Y., Gweon, G.H., Fedorov, A.V., First, P.N., De Heer, W.A., Lee, D.H., Guinea, F., Castro Neto, A.H. and Lanzara, A., *Nat. Mater.*, 2007, 6: 770
- Stankovich, S., Dikin, D.A., Dommett, G.H.B., Kohlhaas, K.M., Zimney, E.J., Stach, E.A., Piner, R.D., Nguyen, S.T. and Ruoff, R.S., *Nature*, 2006, 206: 282
- Wang, S.R., Tambraparni, M., Qiu, J.J., Tipton, J., and Dean, D., *Macromolecules*, 2009, 42: 5251
- Rafiee, M.A., Rafiee, J., Wang, Z., Song, H.H., Yu, Z.Z. and Koratkar, N., *ACS Nano*, 2009, 3(12): 3884
- Wang, J.Q. and Han, Z.D., *Polym. Adv. Technol.*, 2006, 17: 335-340
- Uhl, F.M., Yao, Q., Nakajima, H., Manias, E. and Wilkie, C.A., *Polym. Degrad. Stab.*, 2005, 89: 70
- Li, Z.Z. and Qu, B.J., *Polym. Degrad. Stab.*, 2003, 81: 401
- Shi, L., Li, Z.M., Xie, B.H., Wang, J.H., Tian, C.R. and Yang, M.B., *Polym. Int.*, 2006, 55: 862

- 12 Higginbotham, A.L., Lomeda, J.R., Morgan, A.B. and Tour, J.M., *ACS Appl. Mater. Interfaces*, 2009, 1(10): 2256
- 13 Dasari, A., Yu, Z.Z., Mai, Y.W., Cai, G.P. and Song, H.H., *Polymer*, 2009, 50: 1577
- 14 Staudenmaier, L., *Ber. Dtsch. Chem. Ges.*, 1898, 31: 1481
- 15 Schniepp, H.C., Li, J.L., McAllister, M.J., Sai, H., Herrera-Alonso, M., Adamson, D.H., Prud'homme, R.K., Car, R., Saville, D.A. and Aksay, I.A., *J. Phys. Chem. B*, 2006, 110: 8535
- 16 Matsuo, Y., Tahara, K. and Sugie, Y., *Carbon*, 1996, 34: 672
- 17 Uhl, F.M. and Wilkie, C.A., *Polym. Degrad. Stab.*, 2004, 84: 215
- 18 Matsuo, Y., Tahara, K. and Sugie, Y., *Carbon*, 1997, 35: 113
- 19 Stankovich, S., Piner, R.D., Chen, X., Wu, N., Nguyen, S.T. and Ruoff, R.S., *J. Mater. Chem.*, 2006, 16: 155
- 20 Wang, G., Wang, B., Park, J., Yang, J., Shen, X. and Yao, J., *Carbon*, 2009, 47: 68
- 21 Mao, Y. and Gleason, K.K., *Langmuir*, 2004, 20: 2484
- 22 Vandijkwolthuis, W.N., Franssen, O., Talsma, H., Vansteenbergen, M.J., Vandenbosch, J.J. and Hennink, W.E., *Macromolecules*, 1995, 28: 6317
- 23 Bourlinos, A.B., Gournis, D., Petridis, D., Szabo, T., Szeri, A. and Dekany, I., *Langmuir*, 2003, 19: 6050
- 24 Du, X.S., Yu, Z.Z., Dasari, A., Ma, J., Mo, M., Meng, Y.Z. and Mai, Y.W., *Chem. Mater.*, 2008, 20: 2066